A MORPHOMETRIC STUDY OF THE REMOVAL OF PHENOBARBITAL-INDUCED MEMBRANES FROM HEPATOCYTES AFTER CESSATION OF TREATMENT

ROBERT P. BOLENDER and EWALD R. WEIBEL

From the Department of Anatomy, University of Berne, Berne, Switzerland

ABSTRACT

It is well known that phenobarbital (PB) treatment produces an increase in the amount of cytoplasmic membranes of hepatocytes, with a parallel enhancement in the activity of drug-metabolizing enzymes. However, little is known about how the induced membranes are removed after the drug treatment is stopped. To consider this problem, the recovery of rat hepatocytes from PB induction (five daily injections, 100 mg/kg) was followed morphometrically. Treatment with PB produced a cellular enlargement (26%) due to increases in the volume of the cytoplasmic matrix (20%) and the volume (100%) and surface area (90%) of the smooth-surfaced endoplasmic reticulum (SER). The volume of the nuclei and the surface area of the Golgi apparatus were also increased, but no changes were detected in the volumes of the mitochondria or peroxisomes. The SER membranes induced by the PB were removed within 5 days after the end of the treatment period. During this period of membrane removal, we observed an increase in the volume (800%) and number (96%) of autophagic vacuoles without a change in dense bodies. A morphometric analysis of the content of the autophagic vacuoles showed that the endoplasmic reticulum membranes were preferentially removed, and from this we conclude that the formation of autophagic vacuoles was not a random process. Our findings show that the removal of excess cytoplasmic membranes is associated with an increase in autophagic activity and thus demonstrates the presence of a specific cellular mechanism which may be responsible for the bulk removal of PB-induced membranes.

INTRODUCTION

As shown by many workers (1, 2, 3, 4), the administration of phenobarbital (PB)[1] induces a substantial increase in the cytoplasmic membranes of liver cells, with a parallel enhancement in the activity of drug-metabolizing enzymes. Using a combination of morphometry and biochemistry, Stäubli et al. (4) demonstrated a colinearity between the poliferation of smooth-surfaced membranes (SER) of the endoplasmic reticulum (ER) and the increase in the activity of their constitutive drug-metabolizing enzymes.

Orrenius and Ericsson (5) reported that during the recovery period, i.e. after the drug is withdrawn and the hepatocytes are returning to their

[1] *Abbreviations used in this paper:* AV, autophagic vacuoles; CM, cytoplasmic matrix of hepatocytes; DB, dense bodies; ER, endoplasmic reticulum; GA, Golgi apparatus; gbw, grams per body weight; Mi, mitochondria; NADPH, nicotinamide adenine dinucleotide; PB, phenobarbital; PLP, phospholipid; POCOSTER, Point Counting Stereology Program; Px, peroxisomes; RER, rough-surfaced endoplasmic reticulum; SER, smooth-surfaced endoplasmic reticulum. For morphometric notation, lower case letters are used.

normal condition, the membranes persisted in the hepatocyte cytoplasm for as long as 15 days, while the regression phase for the induced enzymes was only 5 days. Kurijama et al. (6), using rats treated with PB for 8 days, reported a parallel decrease for both microsomes and nicotinamide adenine dinucleotide (NADPH) cytochrome *c* reductase activity during the recovery period, which lasted for about 8 days. In the former case, it would appear that the enzymes are removed before the membranes, whereas in the latter both the enzymes and membranes seemed to be removed at the same time.

The purpose of this report is to describe quantitatively the structural events which lead to the removal of PB-induced membranes on the basis of a morphometric study of intact liver cells. In using this approach it was possible not only to determine the time needed by the cell to reduce its cytoplasmic membrane population to the normal level, but also to obtain new evidence for the role of the lysosomal system, particularly of autophagic vacuoles, in this remodeling process.

MATERIALS AND METHODS

Experimental Procedure

25 adult male albino rats of the same Wistar-derived strain used in previous work from our laboratory (4, 7), weighing between 210 and 300 g, were treated for 5 consecutive days with daily intraperitoneal injections of Na-PB at a dose of 100 mg/kg body weight. The injections were done at 9:00 a.m. with the drug dissolved in 0.9% NaCl. Five control animals received an equivalent volume of 0.9% NaCl.

The animals were sacrificed in groups of five at 1, 2, 3, 5, and 7 days after the last PB injection (cf. Fig. 11); controls, 1 day after the last NaCl injection. They were starved 24 h before sacrifice at which time a deep anesthesia was induced by an intramuscular injection of Hypnorm (fluanisonum/fentanylum) at a dose of 2 mg/kg body weight, after a 30 min pretreatment with Valium (7-chloro-1,3-dihydro-1-methyl-5-phenyl-2*H*-1,4-benzodiazepin-2-one) and Pethidin (pethidinum hydrochloricum). A laparotomy was performed and the liver quickly removed and weighed. Liver volume was determined by dividing liver weight by the density of liver, 1.067 g/cm^3.

Preparation of Tissue for Electron Microscopy

A slice of liver tissue was taken from the medial lobe of the liver, cut into 0.5 mm blocks, and fixed for 2 h at 0°C in 1% osmium tetroxide buffered at pH 7.4 with 0.05 M potassium phosphate, having an osmolality of 340 mosmol. The blocks were then washed for 45 min in cold 0.05 M maleate-NaOH buffer at a pH of 5.2, placed for 2 h in 0.5% uranyl acetate dissolved in the same buffer, and finally washed in maleate buffer for 30 min (8, 9). The tissue blocks were dehydrated in increasing concentrations of cold ethanol, followed by propylene oxide, and embedded in Epon (10).

Sections, having an interference color of silver to gray, were cut on a Reichert ultramicrotome and mounted on 200-mesh copper grids covered with a carbon-coated parlodion film. They were stained with lead citrate (11) for 10–20 min. The preparations were examined in a Philips 300 electron microscope and fields systematically selected (12) were recorded on 35 mm film. Contact prints of these films were projected onto a screen carrying a stereological test system (12).

Sampling

The sample for each time point comes from five animals. Five blocks and, subsequently, five sections were taken from each animal, and seven pictures from each section at each of two different magnifications. This gave a total of 35 pictures per animal, or 175 pictures per time point at each of the two sampling stages.

In the first sampling stage, at a magnification of ~4,500 (primary magnification ~370), estimates were made for the volume densities (cubic centimeter/cubic centimeter) of the extrahepatocytic compartment,[2] and the hepatocyte, including the nuclear and cytoplasmic compartments. The second sampling stage, at a magnification of ~80,000 (primary magnification ~6,700), was used to estimate the volume densities (V_{Vi}; cubic centimeter/cubic centimeter) of the rough (RER)- and smooth (SER)-surfaced endoplasmic reticulum, mitochondria (Mi), peroxisomes (Px), autophagic vacuoles (AV), dense bodies (DB), and cytoplasmic matrix (CM), as well as the surface densities (S_{Vi}; square meter/cubic centimeter) of RER, SER, and Golgi apparatus (GA).

Morphological Criteria for Identifying Components

EXTRAHEPATOCYTIC COMPARTMENT: Endothelial, Kupffer, and fat storing cells were grouped as the extrahepatocytic cellular compartment, while the sinusoidal, Disse, and bile capillary spaces represented the extrahepatocytic space; together they represent the extrahepatocytic compartment (Fig. 1). A de-

[2] The term "compartment" is defined as the aggregate of all the elements of a given component.

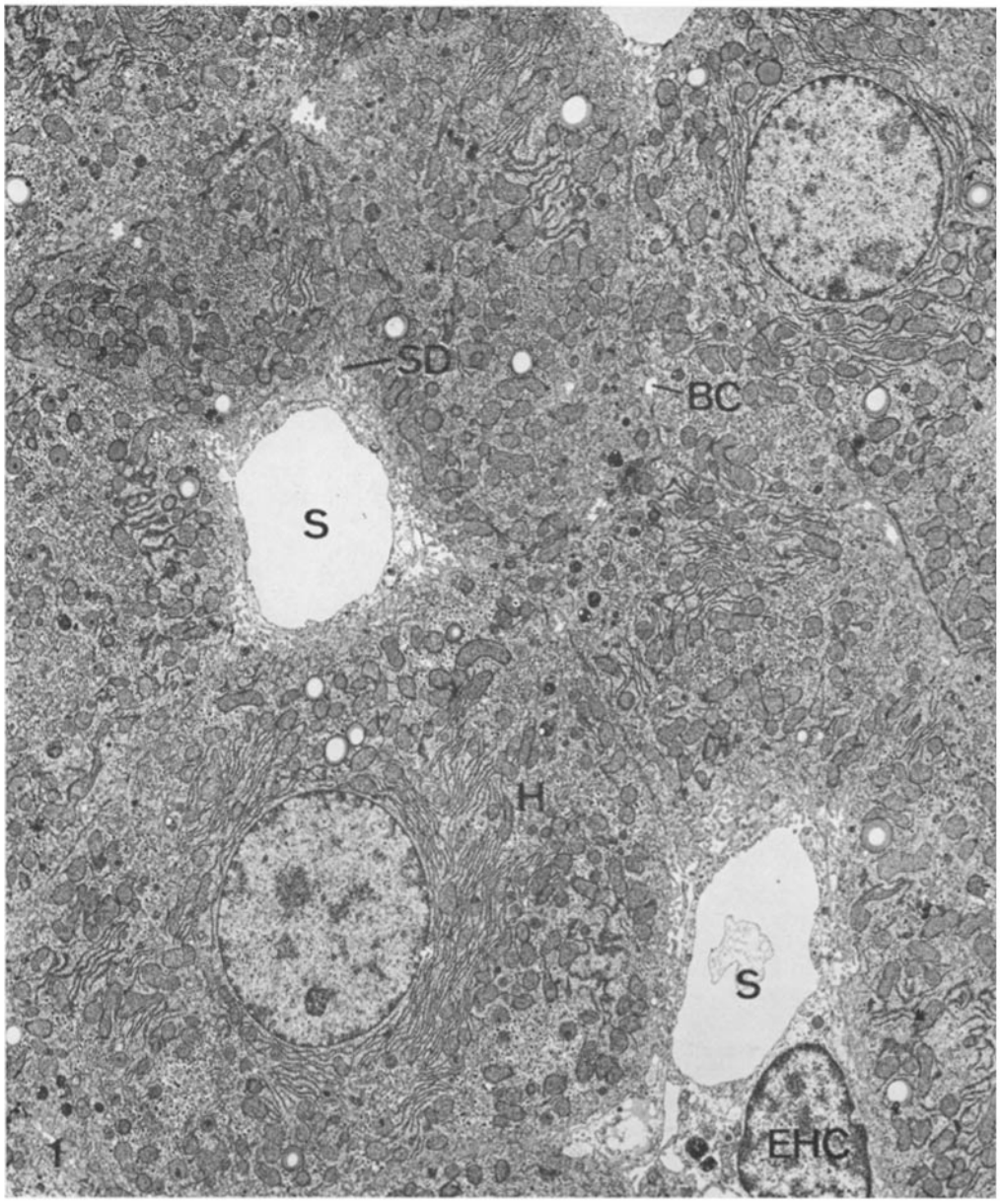

FIGURE 1 Low power micrograph of normal liver showing hepatocytes (*H*), extrahepatocytic cells (*EHC*), sinusoids (*S*), space of Disse (*SD*), and bile canaliculi (*BC*). Used for stage I sampling. × 3,400.

tailed morphometric study of these extrahepatocytic compartments is in preparation.

HEPATOCYTIC COMPARTMENTS: Golgi cisternae and closely associated smooth-surfaced vesicles often containing electron-opaque particles were used to estimate the surface area of the GA (Fig. 2). Px (microbodies) surrounded by a single membrane and having a finely granular matrix frequently displaying a crystalloid are shown in Fig. 3. Mi display both round and oblong profiles and have the characteristic inner and outer membrane structure (Fig. 4). The RER is defined as the group of cytoplasmic membranes, with attached ribosomes, arranged in form of flat cisternae. Membrane profiles within the cisternal stacks lacking ribosomes, the "intercalated areas," were counted with the RER (Fig. 4); in the previous

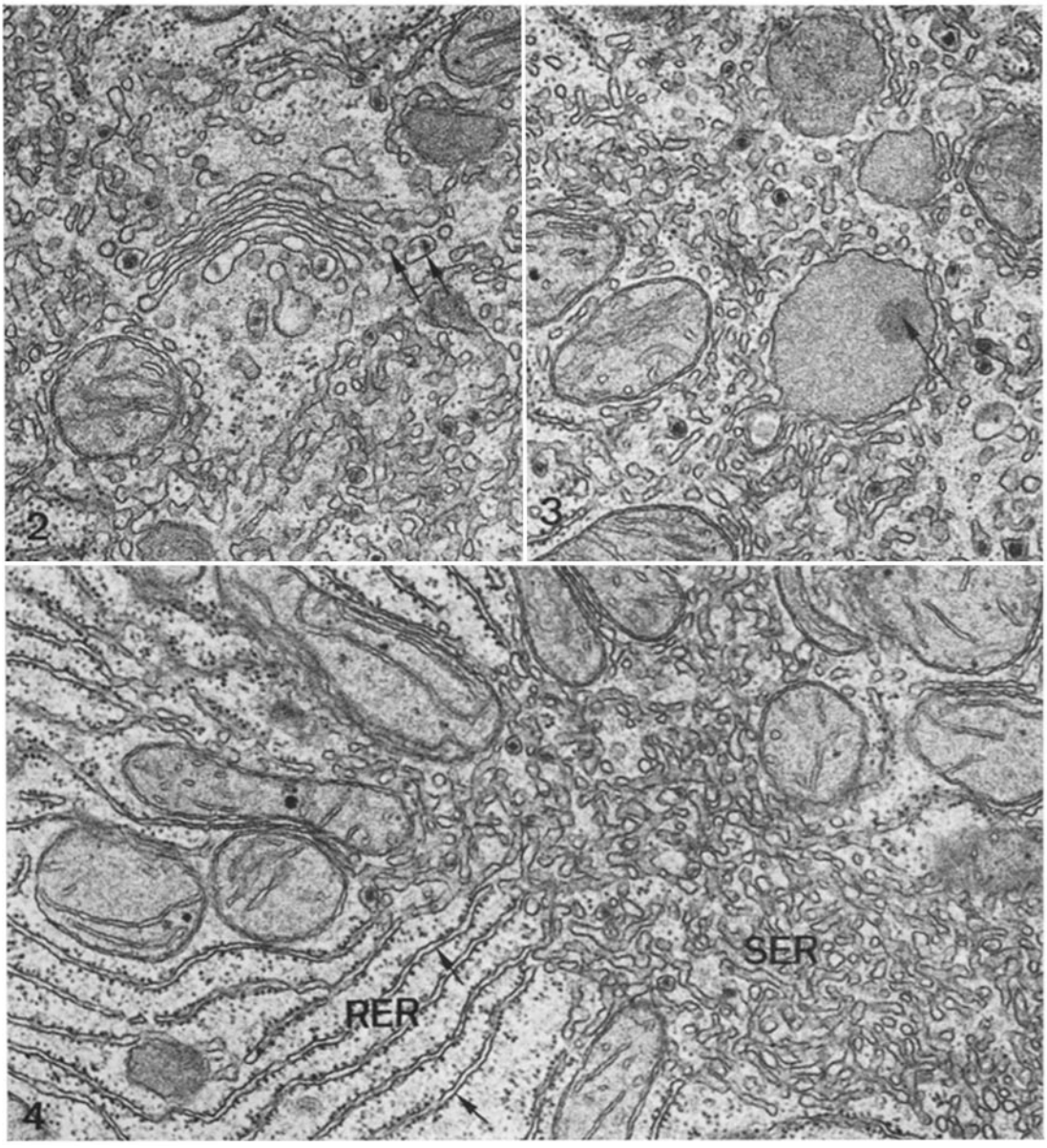

FIGURE 2 GA. An array of smooth-surfaced cisternae and closely associated vesicles (arrows) sometimes containing electron-opaque particles. × 31,000.

FIGURE 3 Px. An organelle surrounded by a single membrane with a homogeneous content often displaying a crystalloid (arrow). × 31,000.

FIGURE 4 Membranes of the ER. The RER consists of those membranes carrying ribosomes and occurring in the form of cisternae. Short sections of membranes devoid of ribosomes but within the RER zones, the "intercalated areas" (arrows), are considered RER. The SER is seen as a tightly meshed network of smooth-surfaced tubules. × 31,000.

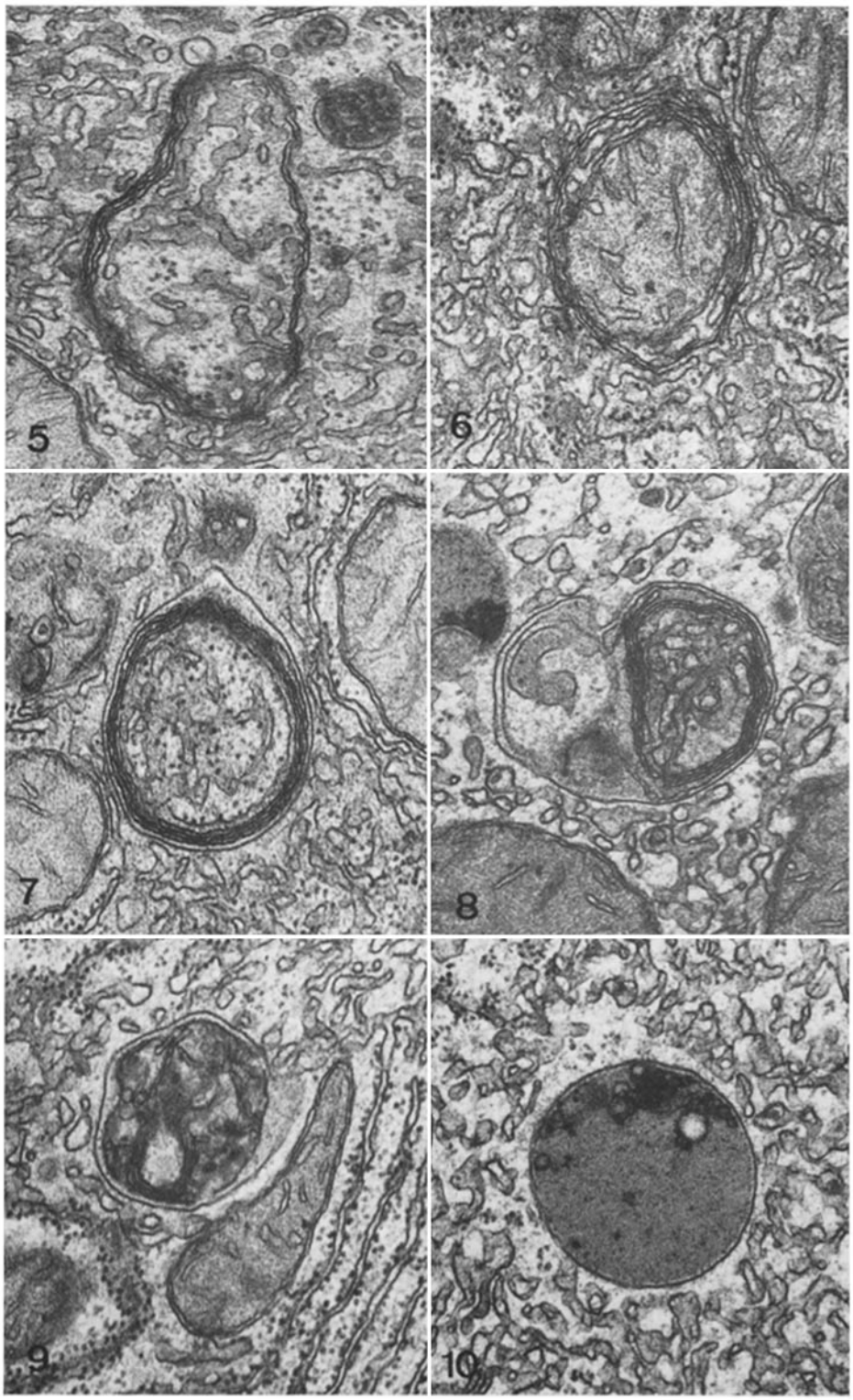

FIGURES 5–10 AV and DB. Figs. 5–9 show what is thought to represent various stages in the development of AV beginning with the sequestration of cytoplasm (Fig. 5), and continuing with progressive changes in the content due, presumably, to the activity of hydrolases (Figs. 6–9). A DB is shown in Fig. 10. × 49,000.

papers (4), these areas had been counted with the SER. The SER is defined as a tightly meshed network of smooth-surfaced tubules and is illustrated in Fig. 4. The criteria for identifying AV as described by Deter (13) were adopted; however, for the present purposes, all the vacuole types were considered as a single group. Vacuole profiles displayed either single-or multiple-limiting membranes and contained cytoplasmic organelles in various stages of digestion (Figs. 5–10). The remaining cytoplasmic components, namely lipid droplets and ground substance, were included in the CM.

Stereological Procedures

TEST SYSTEM: In both sampling stages, the multipurpose test system (12) which contained 84 lines/168 points on a field of 729 cm^2 was used. Estimates were made for volume density by counting points lying over components and for surface density by counting the number of intersections between the test lines and the membrane traces (14).

CALCULATIONS AND STATISTICAL TREATMENT OF RESULTS: Computations were performed with a Hewlett-Packard table top calculator, model 9100 B, and a BULL Gamma 30S digital computer using the POCOSTER computer program of Gnägi (15). The stereological parameters were calculated in terms of densities[3] and specific values which relate volume, surface, and number per 100 g body weight (specific dimensions). While the specific values are reported in this paper, the densities are easily obtained by dividing the specific values by the specific dimension factor[4] (Table I). The formulas used to estimate stereological parameters are outlined in previous work from this laboratory (4, 7).

For each parameter, the mean and the standard error of the mean were calculated; for group comparisons, Student's *t*-test was applied. Two means were considered significantly different if the probability of error, *P*, was less than 0.05. The mean nuclear diameter was estimated by measuring, on very low power electron micrographs, major axes of nuclear profiles, forming 15-size classes, and applying the Wicksell (16) and Giger-Riedwyl (17) procedures to estimate the parameters of the true size distribution of nuclei. Since the measurements were made on thin sections (6–700 Å), no correction was made for section thickness.

RESULTS

Changes in Liver Composition

PB treatment produced an increase in liver volume at days +1, +2, and +3; at days +5 and +7 the liver volume was reduced to within the range of the controls (Table I). In Fig. 11, where the volume changes in the major liver compartments (nuclei and cytoplasm of hepatocytes and extrahepatocytic cells and spaces) are plotted against time, it can be seen that the major increase in liver volume is due to an increase in the volume of the cytoplasmic compartment of hepatocytes (Table I). The increase persisted for 2 days and was then reduced to control levels at days +5 and +7.

Nuclear Changes

Induction with PB did not produce an increase in the nuclear volume when compared to the controls (Table I). However, an increase in volume was seen between days +1 and +3 ($P < 0.02$) followed by a decrease at day +5 ($P < 0.01$). Estimates of mean nuclear diameter using the Wicksell (16) and Giger-Riedwyl (17) procedures are reported in Table II, and, wherever possible, compared to the data of Stäubli et al. (4). It can be seen that the mean diameter of the control nuclei obtained with the Wicksell procedure produced estimates similar to those of the previous study; however, both estimates were somewhat below those coming from numerical density (7), or the Giger-Riedwyl procedure (Table II). Apparently, this is a characteristic feature of the Wicksell transformation (18). Our estimates for the nuclear volume of control animals, coming either from point counting (0.2128 cm^3/100 g per body weight [gbw]) or a mean diameter (8.36 μm) were higher than those of Stäubli et al. (4) (0.1675 cm^3/100 gbw; 7.93 μm) and would explain why we were unable to find the increase they reported at the end of the induction period. However, at the end of the induction period, day +1, both estimates were similar: 0.1991 cm^3/100 gbw compared to 0.2125 cm^3/100 gbw of Stäubli et al. (4). While the reason for this variation is unknown, perhaps it may be traced to the different ages of the animals.

Cytoplasmic Changes

VOLUME OF THE ER: The volume of the cytoplasm of parenchymal cells treated with PB for 5 days increased by 26% which represents a gain of 0.61 ml/100 gbw (Fig. 11). Of this increase, 0.26 ml could be attributed to the ER and the remaining to the CM. Practically all of the increase in ER was due to a hypertrophy of the SER

[3] The densities represent a volume, surface, or number relative to a containing volume.

[4] The specific dimension factor relates liver volume to 100 gbw: $SDF = (V_L)/(W_R) \times 100$.

Table I: Specific values for rat liver

Component	Parameter	Symbol	Days after phenobarbital treatment						Dimension
			Control	+1	+2	+3	+5	+7	per 100 gbw
Animal	Weight	W_R	258.00 *8.60*	288.00 * *4.90*	234.00 *8.72*	246.00 *2.45*	250.00 *3.16*	262.00 *5.83*	g
Liver	Volume	V_L	7.21 *0.51*	9.66 † *0.32*	7.70 *0.56*	8.98 * *0.41*	7.57 *0.19*	7.17 *0.24*	cm^3
Specific Dimension Factor		SDF	2.79 *0.18*	3.36 * *0.15*	3.29 *0.18*	3.65 § *0.16*	3.01 *0.07*	2.77 *0.06*	cm^3
Extrahepatocytic cells and spaces	Volume	V_x	0.4870 *0.0723*	0.4514 *0.0153*	0.5553 *0.0315*	0.5815 *0.0363*	0.6426 *0.0604*	0.5090 *0.0381*	cm^3
Hepatocytes	Volume	V_h	2.3049 *0.1085*	2.9116 † *0.1486*	2.7345 *0.1633*	3.1178 ¶ *0.1461*	2.3634 *0.0646*	2.2630 *0.0683*	cm^3
Nuclei	Volume	V_n	0.2079 *0.0183*	0.1991 *0.0135*	0.2162 *0.0183*	0.2434 *0.0067*	0.1942 *0.0115*	0.1902 *0.0093*	cm^3
Cytoplasm	Volume	V_{cy}	2.0970 *0.0935*	2.7134 § *0.1367*	2.5184 * *0.1487*	2.8744 ¶ *0.1412*	2.1692 *0.0613*	2.0728 *0.0596*	cm^3
Cytoplasmic matrix	Volume	V_{cm}	1.0500 *0.0336*	1.2610 * *0.0668*	1.2160 *0.0936*	1.3720 § *0.0527*	1.1290 *0.0329*	1.0760 *0.0230*	cm^3
Endoplasmic Reticulum	Volume	V_{er}	0.4350 *0.0525*	0.6989 † *0.0572*	0.6510 * *0.0470*	0.6530 * *0.0520*	0.3804 *0.0269*	0.3334 *0.0200*	cm^3
	Surface	S_{er}	24.1300 *1.3200*	37.5700 † *2.8190*	36.5600 * *3.7350*	37.2800 † *2.6970*	26.6300 *1.6200*	25.0000 *1.4620*	m^2
Rough-surfaced ER	Volume	V_{rer}	0.1930 *0.0249*	0.2183 *0.0126*	0.2639 *0.0204*	0.2377 *0.0156*	0.1325 *0.0154*	0.1277 *0.0574*	cm^3
	Surface	S_{rer}	10.9900 *0.3253*	13.2300 * *0.6651*	15.3400 *1.8730*	14.1600 ‡ *0.6942*	10.3400 *0.9401*	10.4700 *0.5626*	m^2
Smooth-surfaced ER	Volume	V_{ser}	0.2419 *0.0294*	0.4806 † *0.0461*	0.3871 † *0.0296*	0.4153 * *0.0612*	0.2479 *0.0251*	0.2057 *0.0217*	cm^3
	Surface	S_{ser}	12.2500 *1.1760*	23.2700 † *2.3620*	20.0900 * *2.0780*	21.6900 * *2.7500*	15.4500 *1.7560*	13.7300 *1.6740*	m^2
Golgi apparatus	Surface	S_{ga}	0.8854 *0.1047*	1.0640 *0.3214*	1.1270 *0.2213*	1.4210 * *0.1824*	0.8330 *0.2131*	0.7861 *0.1712*	m^2
Mitochondria	Volume	V_{mi}	0.5445 *0.0714*	0.6807 *0.0839*	0.5820 *0.0294*	0.7628 *0.0667*	0.6030 *0.0389*	0.5634 *0.0219*	cm^3
Peroxisomes	Volume	V_p	0.0421 *0.0063*	0.0455 *0.0055*	0.0411 *0.0014*	0.0474 *0.0057*	0.0462 *0.0035*	0.0486 *0.0059*	cm^3
Autophagic Vacuoles	Volume	V_{av}	0.00102 *0.00058*	0.00484 *0.00173*	0.00620* *0.00185*	0.00503 *0.00181*	0.00853* *0.00307*	0.00226 *0.00103*	cm^3
	Number	N_{av}	1.284 *0.640*	2.519 *0.997*	5.005 † *1.175*	3.856 *0.937*	3.954 *1.354*	1.322 *0.639*	$x10^{10}$
	Average Volume	$\bar{V}_{av}$	0.048 *0.022*	0.249 *0.130*	0.125 *0.031*	0.152 *0.049*	0.207 *0.014*	0.113 *0.063*	$x10^{-12} cm^3$
Dense bodies	Volume	V_{db}	0.0089 *0.0010*	0.0068 *0.0022*	0.0114 *0.0029*	0.0094 *0.0016*	0.0064 *0.0016*	0.0115 *0.0029*	cm^3
	Number	N_{db}	19.042 *3.600*	15.980 *2.683*	22.768 *3.121*	26.051 *7.906*	14.577 *3.203*	19.420 *2.480*	$x10^{10}$
	Average Volume	$\bar{V}_{db}$	0.055 *0.014*	0.049 *0.015*	0.051 *0.012*	0.043 *0.007*	0.043 *0.004*	0.056 *0.010*	$x10^{-12} cm^3$

Levels of significance, compared to control:

* 0.05
† 0.025
§ 0.01
¶ 0.005
‡ 0.001

Standard errors of the mean indicated in italics.

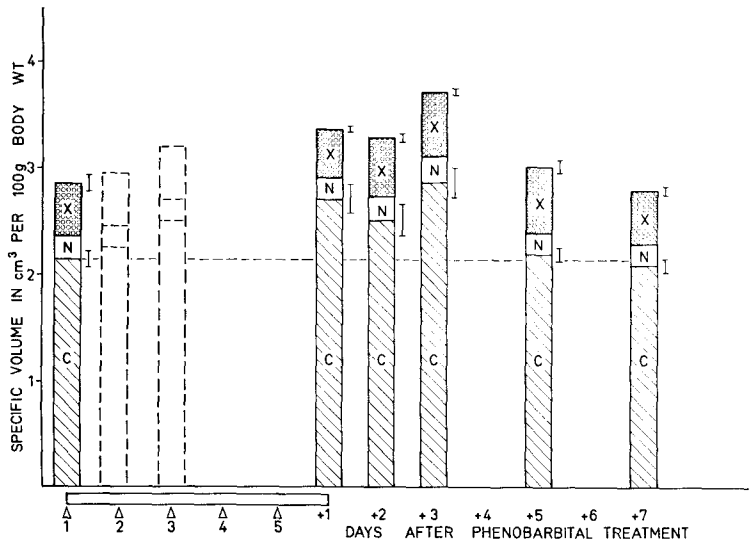

FIGURE 11 Changes in specific liver volume related to changes in hepatocytic and extrahepatocytic compartments. The horizontal bar represents the period of treatment with PB, and the triangles the five daily injections; the plus numbers represent the days after PB treatment. The portion of the vertical bars marked *X* represents the volume of the extrahepatocytic compartment, *N* the nuclear compartment, and *C* the cytoplasmic compartment of hepatocytes. The dashed bars represent data adapted from Stäubli et al. (4). In the cytoplasmic compartment there was a difference between the control and days +1 and +3 (see Table I). Standard errors of the mean for *X* and *C* are indicated.

TABLE II

Estimates of Mean Nuclear Diameters

Days after treatment	Nuclear diameters (μm) After Wicksell (16)	After Giger and Riedwyl (17)	Number of profiles measured
Control	8.02 7.93*	8.36 *1.06*	1144
+1	8.24 8.03*	8.69 *1.40*	1140
+2	8.75	8.98 *1.25*	1181
+3	8.29	8.91 *1.32*	1201
+5	7.34	8.57 *1.28*	904
+7	7.82	8.56 *1.12*	1318

Standard error of the mean is indicated by italics.
* Data from Stäubli et al. (4).

(0.24 ml, a 100% increase) while the augmentation of RER volume by 0.02 ml was not significant (Fig. 12).

The volume of CM and ER remained constant at the induced level for 3 days after completion of the injections (days +1, +2, +3), returning to the control level at days +5 and +7. Although the RER did not increase above the controls during the induction period, it was found to be somewhat below the induced level at days +5 and +7 (Fig. 12). These data indicate that PB produced an increase in the volumes of the CM and the SER which returned to the control levels within 5 days after cessation of the treatment.

SURFACE AREA OF THE ER: The changes in the specific surface area of the ER generally paralleled those of the specific volumes (Table I; Figs. 12, 13). At day +1, the surface area of the ER was found to be increased to 60% above the control value of 24.1 m^2/100 gbw; it persisted at this level for the next 2 days (+2 and +3), and returned to the control level by day +5. As was the case for the volumes, the SER was the primary contributor to these increases. At day +1 the surface area of the SER went from a control

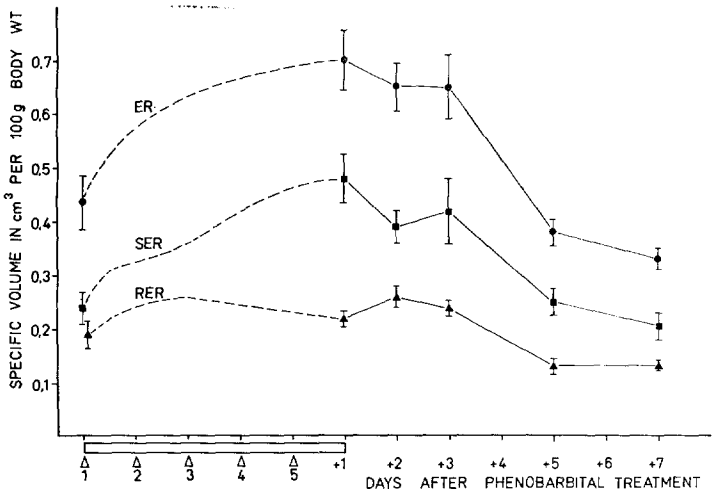

FIGURE 12 Changes in the specific volumes of the ER. The dashed lines represent data adapted from Stäubli et al. (4). Differences between the control and subsequent days were seen for the ER and SER at days +1, +2, and +3 (see Table I). During the recovery period, differences were found between day +3 and +5 for the ER ($P < 0.01$), RER ($P < 0.01$), and SER ($P < 0.05$); and between days +3 and +7 for the ER ($P < 0.001$), RER ($P < 0.001$), and SER ($P < 0.05$) (Table I). Standard errors of the mean are indicated; see Table I for levels of significance.

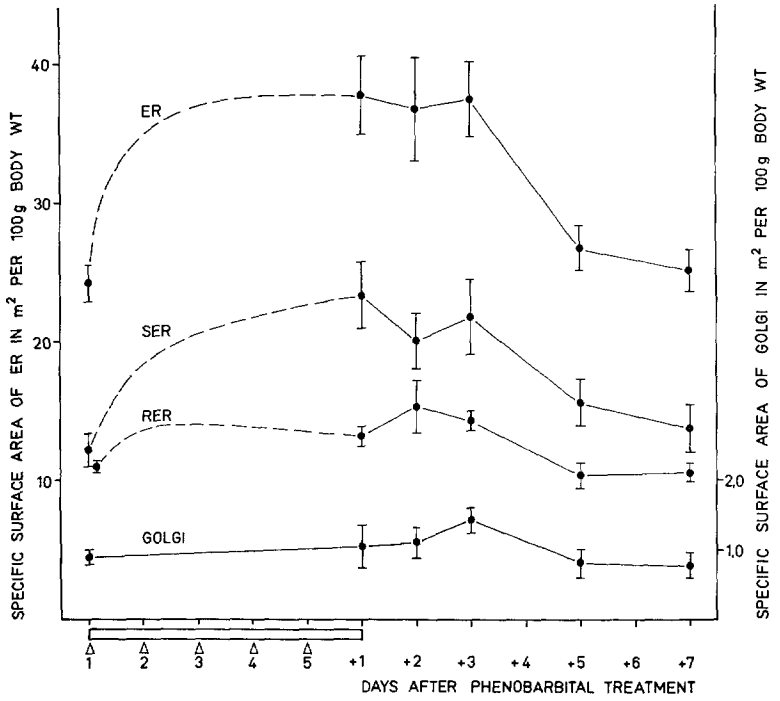

FIGURE 13 Changes in the specific surface area of the ER and the GA. The dashed lines represent data adapted from Stäubli et al. (4). Differences between the control and subsequent days were seen for the ER and SER at days +1, +2, and +3; for the RER at days +1 and +3; and for the GA at days +3. During the recovery period, differences were found between days +3 and +5 for the ER ($P < 0.01$), and RER ($P < 0.05$); and between days +3 and +7 for the ER ($P < 0.01$), RER ($P < 0.01$), SER ($P < 0.05$), and the GA ($P < 0.05$). Standard errors of the mean are indicated; see Table I for levels of significance.

value of 12.3 m^2/100 gbw to 23.3 m^2/100 gbw, a 90% increase. This induced level was maintained until day +3, falling to 15.5 m^2/100 gbw at day +5 and 13.7 m^2/100 gbw at day +7, values not significantly different from the controls. The surface area of the RER changed to a lesser extent, increasing by about 25% from a control value of 11.0 m^2/100 gbw to 13.2 m^2/100 gbw, 15.3 m^2/100 gbw, and 14.2 m^2/100 gbw at days +1, +2, and +3, respectively. A return of the RER to the control levels was found at day +5 (10.3 m^2/100 gbw) and day +7 (10.5 m^2/100 gbw).

SURFACE AREA OF THE GA: The surface area of the GA, 0.89 m^2/100 gbw in the controls, was significantly elevated only at day +3 (Table I, Fig. 13).

VOLUME OF MI AND PX: No differences were detected between the control and subsequent points for either Mi or Px (Table I, Fig. 14).

VOLUME AND NUMBER OF DB: No differences were observed between any of the points coming from estimates of volume (Fig. 16), number, or average volume of DB (Table I). The control values were 0.0089 cm^3/100 gbw for volume, 19.04 × 10^{10}/100 gbw for number, and 0.055 × 10^{-12} cm^3 for average size.

VOLUME AND NUMBER OF AV: The volume of the AV was greater than the controls (0.0010 cm^3/100 gbw) at days +2 (0.0062 cm^3/100 gbw) and +5 (0.0085 cm^3/100 gbw) (Fig. 15, Table I). Only at day +2 (5.005 × 10^{10}/100 gbw) was the number of AV greater than the control (1.284 × 10^{10}/100 gbw) (Table I). The size of an average vacuole is increased during the recovery period, compared to the controls, but, because of the broad size ranges, a significant difference can be seen only at day +5 where there is a narrower size distribution.

DISCUSSION

Methods

The methods of this paper generally follow those outlined by Weibel et al. (7) and Stäubli et al. (4); however, a few modifications were introduced. During the fixation procedure, contrast was enhanced with en bloc staining which made it easier to identify membrane profiles. Light microscope observations were replaced with observations made on very low power electron micrographs recorded with the "scanning" position of the Philips EM 300, thereby requiring only one set of ultrathin sections (6–700 Å) for all sampling levels. Furthermore, the use of ultrathin sections for the low magnifications obviated the difficult task of making corrections for section thickness in estimating nuclear diameters, and greatly facilitated the identification of cellular compartments and extracellular spaces.

Controls

The estimate for mean nuclear diameter using the Wicksell transformation (16) was similar to that of the previous study (7; Table II). Our primary measurements of the diameters of nuclear profiles were made on very low power electron micrographs and, consequently, did not require the complicated correction for section thickness, necessary when these measurements are made on

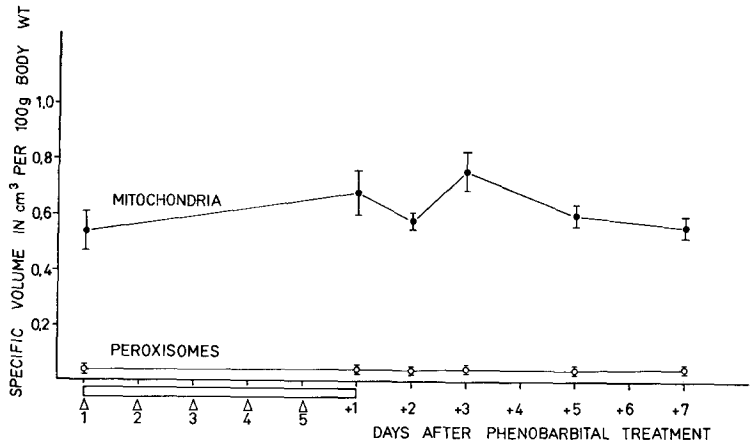

FIGURE 14 Specific volumes of Mi and Px. Standard errors of the mean are indicated; an increase in volume of Mi was found between days +2 and +3 ($P < 0.05$).

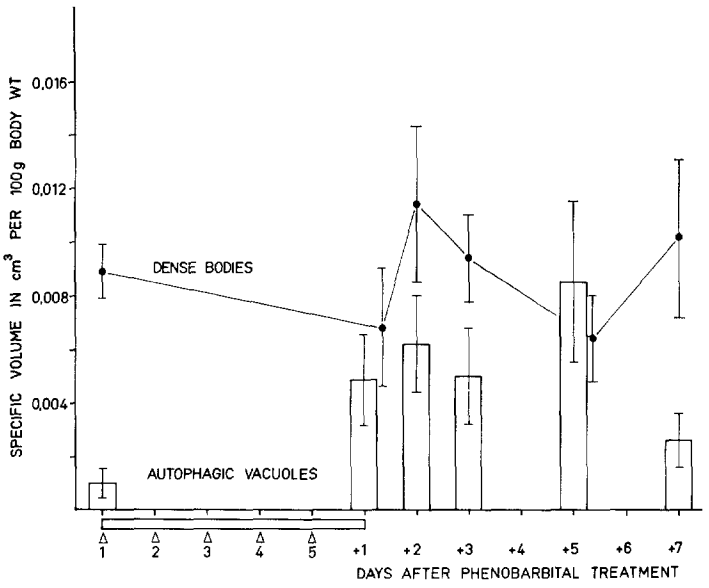

FIGURE 15 Changes in the specific volume of AV (histogram) and DB (line). Differences between the control and subsequent days were seen for the AV at days +2 and +5; no differences were found for the DB (Table I). Standard errors of the mean are indicated.

thick sections ($\sim 2\ \mu$m), in the previous study (4). The Wicksell transformation was, therefore, easily performed with a programmable table top calculator. The semigraphic Giger-Riedwyl method (17), used to estimate mean nuclear diameters, is based on the assumption that the nuclei are spherical and normally distributed. The method is particularly useful in that it corrects for lost profiles (cap sections), provides standard deviations, and is simple to apply.

Our estimate for the surface area of the ER membranes was 8.6 m^2/ml of liver or 10.7 m^2/ml when multiplied by 1.25, a somewhat arbitrary correction for undetected membranes (7). In the first morphometric study of the liver, Loud (19) reported 4.3 m^2/ml, or, when corrected with a factor of 1.5, 6.5 m^2/ml of liver. Weibel et al. (7) reported 10.9 m^2/ml of liver, or corrected 13.6. A unique determination comes from Wibo et al. (20) who estimated the surface area of the ER by a combined stereological-biochemical method, and their corrected value was 7.9 m^2/ml of liver. However, their ER preparation, resulting from liver homogenization, contained Golgi membranes which, according to our estimates, would amount to 0.3 m^2/ml of liver. Moreover, their ER fraction was contaminated by nonparenchymal sources, primarily Kupffer and endothelial cells. The data are thus not strictly comparable. It appears, however, that there are some differences in the estimates of ER surface in the rat liver, the reasons for which must be clarified by future work, but they should not affect the present study since closely matched internal controls were used.

The components of the lysosomal system in the rat liver, including AV and DB, have been estimated previously. Using cell fractionation techniques, Baudhuin (21) reported for DB a volume of 0.379 cm^3/100 cm^3 of liver and 6.1 $\times$ 10^{10} DB/g of liver; the values were corrected for losses due to fractionation. Our estimates for DB, taken from intact tissue, were 0.33 $\pm$ 0.05 cm^3/100 cm^3 of liver for the volume and 6.91 $\times$ 10^{10}/ml of liver for the number which are in agreement with those of Baudhuin (21). The estimates of Deter (13) were also obtained from tissue fractions but were uncorrected for considerable losses due to the isolation procedure and, consequently, gave lower values: DB volume, 0.184 $\pm$ 0.011 cm^3/100 cm^3 of liver and DB number, 3.07 $\pm$ 0.16 $\times$ 10^{10}/g of liver. Furthermore, the estimate of Deter (13) for the volume of AV, 0.018 cm^3/100 g of liver, was again lower than ours from intact tissue 0.036 $\pm$ 0.021 cm^3/100 cm^3; the same holds true for the number of AV, 0.068 $\times$ 10^{10}/g of liver, and ours, 0.436 $\pm$ 0.208 $\times$ 10^{10}/cm^3 of liver (1 cm^3 of liver = 1.067 g). However, by determining the mean volume of an AV, it can be seen that the

vacuole volume of the Deter study was larger than ours, by about three times. Whether the larger volume of the individual vacuoles was due to the fractionation procedure, or if it truly represented the condition in the intact tissue, was not determined in his study.

PB Induction

In the present experiment we used the same strain of rats but heavier animals than those of Stäubli et al. (4); the control rats in our experiment were 48% heavier with 23% heavier livers giving a specific liver volume, used to relate the various parameters to a standardized body weight, which was 21% lower than in the previous study. However, the relative change in the specific liver volumes under PB treatment is practically the same at day +1, being 1.28 in the younger and 1.26 in the older animals.

We detected an increase in nuclear volume only at day +3 ($P < 0.02$) followed by a decrease at days +5 ($P < 0.01$) and +7 ($P < 0.005$) while Stäubli et al. found an increase at day +1. Although both studies show that PB causes an increase in nuclear volume, we are unable to explain why the increase was seen 2 days later in our experiment. We should hasten to add, however, that while the control volume in our study was greater, the estimates for day +1 were similar for both studies. Although this would account for the statistical differences, it does not explain the larger initial nuclear volume in our study.

After PB treatment, the surface of the ER increased by 56% (13.44 $m^2$100 gbw), that of the SER by 90% (11.02 m^2/100 gbw), as compared to 73% (26.5 m^2/100 gbw) and 256% (24.4 m^2/100 gbw), respectively, in the study of Stäubli et al. (4). The only apparent difference in the experimental protocol of the two studies which could account for an induction differing by a factor of 2 is the difference in the weights (ages) of the animals. If this is the reason for the difference in induction, then animal weight (age) should become an important consideration in PB experiments.

Another variation between the present work and that of Stäubli et al. (4) points to the importance of choosing the appropriate parameter to describe a change in cellular structure. When the ER surface-to-volume ratios of the two studies were compared, it was found that our values were 55% larger. This would suggest that the ER cisternae of the Stäubli study were more dilated, or ours contracted, a difference which may be due to conditions of fixation or, perhaps, to a variation in physiological state (22).

Removal of Membranes during Recovery from PB Treatment

This study has shown for the first time that the ER membranes of PB-treated animals persist at the induced level until 3 days after the last injection, and that they have fallen to control levels on the 5th day. Furthermore, we have demonstrated that an increase in the volume of AV occurs at the same time as a decrease in both the volume and the surface area of the ER. These findings, therefore, would suggest that the removal of the induced membranes is brought about, at least in part, by the formation of cytosegrosomes or AV.

It is believed that the organelles enclosed in AV are rapidly degraded through the action of introduced lysosomal enzymes, the AV eventually being tranformed into cytosomes or DB (23). However, the way in which the hydrolytic enzymes are added to the vacuoles remains uncertain. Using glucagon-induced autophagy, Deter (13) reported an increase in the number of AV associated with a decrease in the number of DB and concluded that the DB were providing the hydrolytic enzymes by fusing with the AV. Studying the same system, Arstila and Trump (24) came to a different conclusion, namely, that the Golgi vesicles rather than the DB were the principal source of the hydrolytic enzymes. In this respect it may be of interest to note that we observed an increased surface of the GA at day +3, just before the phase of ER removal and AV proliferation; DB appeared to be relatively low at day +5, but this value was not significantly different from any other time point due to large scatter of the data.

During the recovery period, we expected that the great increase in the autophagic granule compartment would eventually lead to increases in the DB compartment; however, this was not the case. It may be that an increase in DB was balanced either by a removal from the cytoplasmic compartment by their release into the bile canaliculi and/or by fusion with AV. It should be apparent from the above discussion that in order to describe the dynamic relationship between AV and DB, further information is necessary on the

rates of movements between the various compartments, a line of work we are currently pursuing.

It has been suggested that the formation of AV is a random process (25). If this were the case, then one would expect the volume fraction of the components enclosed within the vacuoles to be the same as that found in the cytoplasm. Accordingly, there should be no difference between the values observed and those expected if randomness is postulated. Knowing the number of points falling on the AV, the numbers of points expected to fall on Mi and ER within AV can be calculated from the volume densities obtained on cytoplasm and the chi-square test applied to compare them with the actual measurements (Table III). With the single exception of day +1, the results strongly reject the hypothesis that the formation of AV is a random process; they rather show that ER membranes and the associated CM are preferentially enclosed in AV, thus favoring the view that AV are formed in a nonrandom fashion specifically aimed at the removal of excess ER membranes.

Comparisons with Biochemical Data

In untreated rats, the rates of membrane synthesis and breakdown are in balance, the hepatocytes being in a state of dynamic equilibrium. However, when the rat is treated with PB, these rates become altered and there is a net increase in the amount of ER membranes. Associated with this increase in membranes is a severalfold increase in some of the enzymes found in normal hepatocytes, namely those of the NADPH-oxidase chain (26, 27, 6). Furthermore, it appears that PB treatment extends the half-lives of microsomal proteins and phospholipids (PLP) from about 2 to 7 days (27, 28, 29).

TABLE III

Chi-Square Test for AV

Days after PB treatment	Points on structures: Observed ER	Observed Mi	Theoretical ER	Theoretical Mi	Chi-square
0	36	6	23	8	7.07
+1	40	11	30	10	3.04
+2	76	0	43	14	37.58
+3	42	5	26	10	11.27
+5	105	5	55	22	56.93
+7	27	4	16	6	7.27

Chi-square was calculated using the Yates correction. For 1° of freedom ,χ^2 = 3.84. The contents of the AV were classified either as Mi or ER, which includes the CM.

During the recovery period, the membranes and constitutive enzymes return to control levels. The time needed for the removal of induced membranes, as estimated from our electron micrographs, was 5 days. In a similar experiment, Orrenius and Ericsson (5) reported that the return of oxidative demethylation activity to control levels occurred also within 5 days. Kurijama et al. (6), using rats treated with PB for 8 days, found a 45 h half-life for the decrease in the excess amount of NADPH-cytochrome *c* reductase which gave a return to control levels within about 8 days. Considering this longer induction period and the close agreement of our morphometric data with the enzyme data of Orrenius and Ericsson (5), where the induction period was identical, it would appear that there is a parallel decrease in the surface area and enzyme activity of the ER during the recovery period.

After eight daily injections of PB, Kurijama et al. (6) obtained an increase in the milligrams of microsomes per gram of liver to 150% of the controls which fell to 130% and 120% at days +5 and +8, respectively. In our study, five daily injections induced an increase in ER volume to 160% and in surface to 156% of the controls which returned to 110% and 103% at days +5 and +7, respectively, both values not being significantly different from the controls. Kurijama et al. (6) did not include a statistical treatment of their data, but in our experiment we found that estimates using five animals gave a SE in the range of ±5–10% of the mean. It is therefore not certain that their value of 120% at day +8 was significantly different from the control. Considering the longer induction period in their experiment (this produced about 20% more excess microsomes per gram of liver than found after only 5 days of PB treatment) and their reported concomitant regression of both enzymes and PLP, their data would tend to support our hypothesis of a parallel removal of membranes and enzymes.

Orrenius and Ericsson (5), on the other hand, measuring milligrams of PLP per gram of liver, found an increase to about 250% during the induction which failed to return to control levels until 2 wk after the treatment with PB was stopped. As a support for this finding of a sustained level of

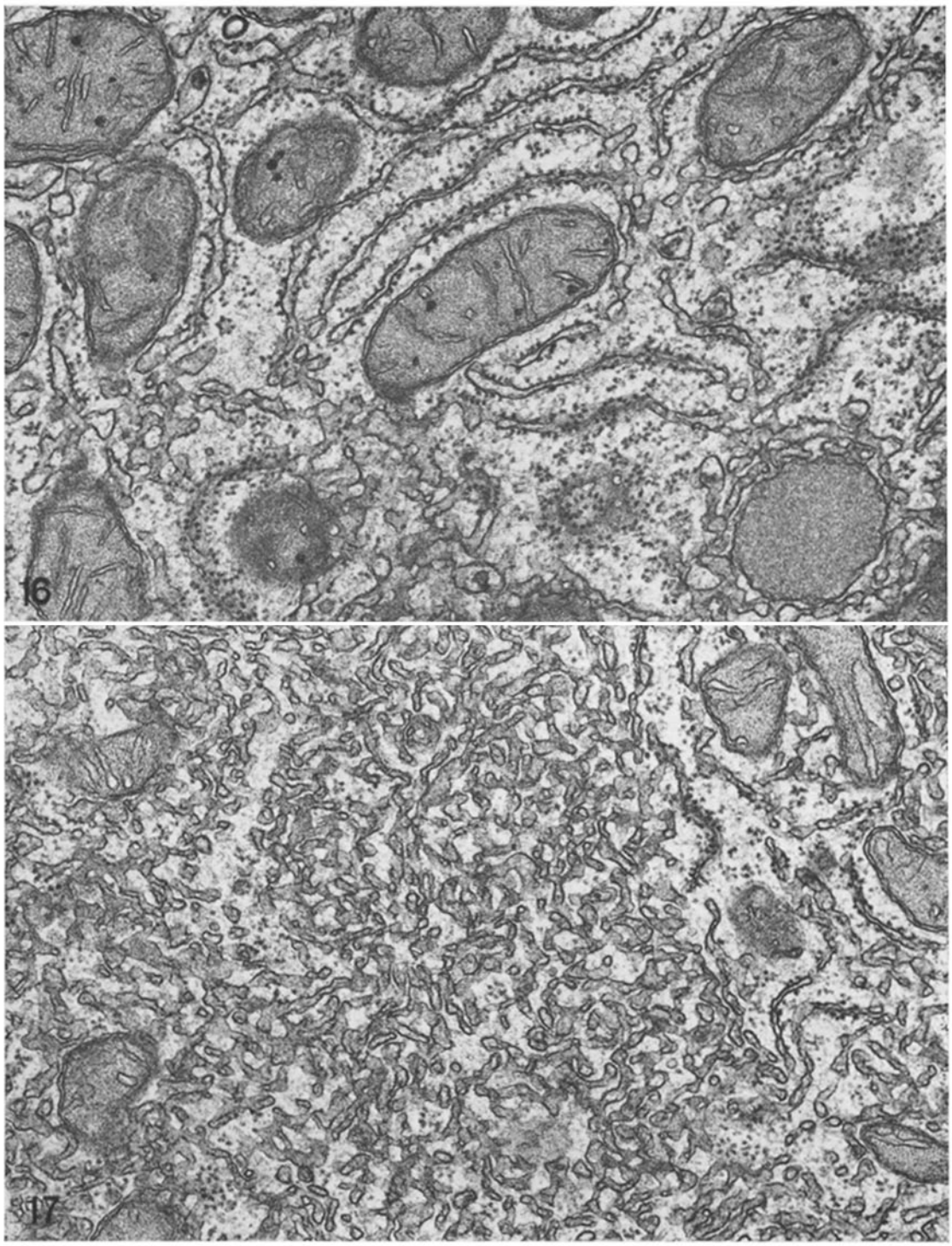

FIGURES 16 and 17 These micrographs are taken from the same animal at day +5 (5 days after the final PB injection), wherein Fig. 16 shows the typical appearance of ER membranes in noninduced rats and Fig. 17 could easily be interpreted as a packet of induced SER. × 47,000.

PLP, they described the presence of an elevated amount of ER membranes throughout the recovery period as seen in electron micrographs. In our similar experiment, we too found scattered areas of membrane concentrations similar to those observed at day +1 (the time of greatest induction) to occur even at days +5 and +7. Micrographs exhibiting the "typical" picture of induced and normal cells taken from the same animal at day +5 are shown in Fig. 16 and 17; that this misleading observation is not representative of the whole liver is shown by our morphometric results. On the basis of the assumption that the induced membranes were still present in the cells at day +5, Orrenius and Ericsson (5) tried to reinduce the excess membranes, but reported that new induction required the synthesis of new ER and not the reuse of preexisting membranes. This observation can be explained by our finding that, in a quantitative sense, there is no excess membrane surface present in the cells at day +5.

It is evident that such controversies could be resolved by combined morphometrical-biochemical studies, a course we are presently pursuing.

The results of our morphometric studies on the effect of PB treatment on cytoplasmic membranes of hepatocytes during the induction (4) and recovery periods can be summarized as follows. Within 16 h after the first injection of PB there was an increase in both the RER and SER, and, while the RER quickly reached a plateau, the SER continued to increase throughout the induction period. When the drug was withdrawn, the SER no longer increased and was maintained at a steady-state level of induction for about 2 more days. The final phase of the recovery occurred during the next 2 days when we observed a larger increase in the amount of AV and a rapid disappearance of the excess ER membranes. This finding demonstrates the presence, in addition to biochemical turnover, of a specific cellular mechanism which may be responsible for the bulk removal of PB-induced membranes.

We wish to thank Miss Margret Fehlmann, Mrs. Rosmarie Bachmann, and Mr. Karl Babl for their skilled assistance and Mr. Hans-Rudolf Gnägi for the computer evaluation of the data.

This work was supported by grant nos. 5261.3 and 3.554.71 from the Swiss National Science Foundation, and by grants from the Sandoz-Stiftung, the Leopold Schepp Foundation, and the American-Swiss Foundation.

Received for publication 31 July 1972, and in revised form 6 October 1972.

REFERENCES

1. Remmer, H., and H. J. Merker. 1965. Effect of drugs on the formation of smooth endoplasmic reticulum and drug-metabolizing enzymes. *Ann. N.Y. Acad. Sci.* **123**:79.
2. Conney, A. H. 1967. Pharmacological implications of microsomal enzyme induction. *Pharmacol. Rev.* **19**:317.
3. Jones, A. L., and D. W. Fawcett. 1965. Hypertrophy of the agranular reticulum in hamster liver induced by phenobarbital (With a review on the functioning of this organelle in liver). *J. Histochem. Cytochem.* **14**:215.
4. Stäubli, W., R. Hess, and E. R. Weibel. 1969. Correlated morphometric and biochemical studies on the liver cell. II. Effect of phenobarbital on rat hepatocytes. *J. Cell Biol.* **41**:92.
5. Orrenius, S., and J. L. E. Ericsson. 1966. Enzyme-membrane relationship in phenobarbital induction of synthesis of drug-metabolizing enzyme system and proliferation of endoplasmic membranes. *J. Cell Biol.* **28**:181.
6. Kurijama, Y., T. Omura, P., Siekevitz, and G. E. Palade. 1969. Effects of phenobarbital on the synthesis and degradation of the protein components of rat liver microsomal membranes. *J. Biol. Chem.* **244**:2017.
7. Weibel, E. R., W. Stäubli, H. R. Gnägi, and F. A. Hess. 1969. Correlated morphometric and biochemical studies on the liver cell. I. Morphometric model, stereologic methods, and normal morphometric data for rat liver. *J. Cell Biol.* **42**:68.
8. Farquhar, M. G., and G. E. Palade. 1965. Cell junctions in amphibian skin. *J. Cell Biol.* **26**:263.
9. Karnovsky, M. J. 1967. The ultrastructural basis of capillary permeability studied with peroxidase as a tracer. *J. Cell Biol.* **35**:213.
10. Luft, J. H. 1961. Improvements in epoxy resin embedding methods. *J. Biophys. Biochem. Cytol.* **9**:409.
11. Reynolds, E. S. 1963. The use of lead citrate at high pH as an electron-opaque stain in electron microscopy. *J. Cell Biol.* **17**:208.
12. Weibel, E. R. 1969. Stereological principles for morphometry in electron microscopic cytology. *Int. Rev. Cytol.* **26**:235.
13. Deter, R. L. 1971. Quantitative characterization of dense body, autophagic vacuole, and acid phosphatase-bearing particle populations

during the early phases of glucagon-induced autophagy in rat liver. *J. Cell Biol.* **48**:473.

14. WEIBEL, E. R., and R. P. BOLENDER. 1973. Stereological techniques for electron microscopic morphometry. *In* Principles and Techniques of Electron Microscopy. M. A. Hayat, editor. Van Nostrand Reinhold Company, New York.
15. GNÄGI, H. R., P. H. BURRI, and E. R. WEIBEL. 1970. A multipurpose computer program for automatic analysis of stereological data obtained on electron micrographs. Proceedings of the 7th International Congress for Electron Microscopy, Grenoble. 443.
16. WICKSELL, S. D. 1925. On the size distribution of sections of a mixture of spheres. *Biometrika.* **17**:84.
17. GIGER, H., and H. RIEDWYL. 1970. Bestimmung der Grössenverteilung von Kugeln aus Schnittkreisradien. *Biom. Z.* **12**:156.
18. BAUDHUIN, P., and J. BERTHET. 1967. Electron microscopic examination of subcellular fractions. II. Quantitative analysis of the mitochondrial population isolated from rat liver. *J. Cell Biol.* **48**:631.
19. LOUD, A. V. 1968. A quantitative stereological description of the ultrastructure of normal rat liver parenchymal cells. *J. Cell Biol.* **37**:27.
20. WIBO, M., A. AMAR-COSTESEC, J. BERTHET, and H. BEAUFAY. 1971. Electron microscope examination of subcellular fractions. III. Quantitative analysis of the microsomal fraction isolated from rat liver. *J. Cell Biol.* **51**:52.
21. BAUDHUIN, P. 1968. L'analyse morphologique quantitative de fractions subcellulaires. Thèse d'Agrégation, University of Louvain, Louvain, Belgium.
22. FAWCETT, D. W. 1961. The membranes of the cytoplasm. *Lab. Invest.* **10**(Suppl.):1162.
23. ERICSSON, J. L. E. 1969. Mechanism of cellular autophagy. *In* Lysosomes in Biology and Pathology. North Holland Publishing Co., Amsterdam. **2**.
24. ARSTILA, A. U., and B. J. TRUMP. 1968. Studies on cellular autophagocytosis. The formation of autophagic vacuoles in liver after glucagon administration. *Am. J. Pathol.* **53**:687.
25. DE DUVE, C. 1964. From cytases to lysosomes. *Fed. Proc.* **23**:1045.
26. CONNEY, A. H., and A. G. GILMAN. 1963. Puromycin inhibition of enzyme induction by 3-methylcholanthrene and phenobarbital. *J. Biol. Chem.* **238**:3682.
27. SHUSTER, L., and H. JICK. 1966. The turnover of microsomal protein in the livers of phenobarbital treated mice. *J. Biol. Chem.* **241**:5361.
28. OMURA, T., P. SIEKEVITZ, and G. E. PALADE. 1967. Turnover of constituents of the endoplasmic reticulum membranes of rat hepatocytes. *J. Biol. Chem.* **242**:2389.
29. HOLTZMAN, J. L., and J. R. GILLETTE. 1968. The effect of phenobarbital on the turnover of microsomal phospholipid in male and female rats. *J. Biol. Chem.* **243**:3020.